

Faraday shields within a solenoidal coil to reduce sample heating: Numerical comparison of designs and experimental verification

BuSik Park^{a,b}, Thomas Neuberger^c, Andrew G. Webb^d, Don C. Bigler^a, Christopher M. Collins^{a,b,*}

^a Department of Bioengineering, The Pennsylvania State University, College of Medicine, Hershey, PA, USA

^b Department of Radiology, The Pennsylvania State University, College of Medicine, Hershey, PA, USA

^c Department of Bioengineering, The Pennsylvania State University, University Park, PA, USA

^d C.J. Gorter High Field Magnetic Resonance Center, Department of Radiology, Leiden University Medical Center, The Netherlands

ARTICLE INFO

Article history:

Received 29 July 2009

Revised 24 September 2009

Available online 4 October 2009

Keywords:

Solenoidal coil

Shield

SAR

Sample heating

ABSTRACT

A comparison of methods to decrease RF power dissipation and related heating in conductive samples using passive conductors surrounding a sample in a solenoid coil is presented. Full-Maxwell finite difference time domain numerical calculations were performed to evaluate the effect of the passive conductors by calculating conservative and magnetically-induced electric field and magnetic field distributions. To validate the simulation method, experimental measurements of temperature increase were conducted using a solenoidal coil (diameter 3 mm), a saline sample (10 mM NaCl) and passive copper shielding wires (50 μ m diameter). The temperature increase was 58% lower with the copper wires present for several different input powers to the coil. This was in good agreement with simulation for the same geometry, which indicated 57% lower power dissipated in the sample with conductors present. Simulations indicate that some designs should be capable of reducing temperature increase by more than 85%.

© 2009 Elsevier Inc. All rights reserved.

1. Introduction

In MRI and high resolution NMR of small samples, the RF electrical fields within the sample can be a significant factor in temperature increase (ΔT) and SNR [1]. The vast majority of MR microscopy and small-volume NMR studies use solenoidal coils. In this geometry, the conservative electric (E_c) field – mainly caused by the scalar electric potential in the coil winding [2] – can be a significant component of the total electric field in the sample [1,3]. This has led to a variety of proposed methods to reduce the E_c field (and associated heating) within the sample while still maintaining a significant B_1 field intensity. These methods have included passive [4,5] or active [6] conductors between the solenoidal coil and the sample, and use of coil geometries other than the solenoid that have significantly lower E_c fields [7–9].

In this paper we use numerical methods to compare some simple methods to decrease sample power loss and related ΔT using strategically-positioned passive conductors to partially shield the sample from the E_c field of the solenoidal coil. We refer to a set of conductors placed between the coil and the sample to shield conservative E-fields while allowing B_1 to penetrate the sample as an “ E_c shield.” Full-Maxwell numerical calculations of the electromagnetic fields

are performed to evaluate several different arrangements of copper strips oriented along the major axis of the solenoid and arranged about the circumference of the cylinder in a manner similar to that described by Gadian [4] and applied recently by Wu and Opella [10], as well as a more recently proposed method, referred to here as the “loop-gap shield” [5]. To validate the numerical calculation method, experiments measuring ΔT with and without a specific E_c shield geometry are performed and results are compared to those from simulations of the same geometry.

2. Theory

The time-rate of change in temperature (dT/dt) within a non-perfused material with an internal heat source, arising from the specific energy absorption rate (SAR) can be written as

$$\frac{dT}{dt} = \frac{1}{\rho c} (\nabla \cdot (k \nabla T) + \text{SAR} \rho) \quad (1)$$

where ρ is the mass density, c the heat capacity, and k the thermal conductivity. The SAR can be calculated as

$$\text{SAR} = \frac{\sigma E_{\text{total}}^2}{2\rho} \quad (2)$$

where σ is the local electrical conductivity of the sample and E_{total} is the magnitude of the total electric field within the sample. E_{total} can be separated into two components, E_c (caused by the spatial distri-

* Corresponding author. Address: NMR/MRI Building, H066, 500 University Drive, Hershey, PA 17033, USA. Fax: +1 717 531 8486.

E-mail address: cmcollins@psu.edu (C.M. Collins).

bution of the scalar electric potential ϕ), and E_i , induced by the time-varying magnetic fields. This can be expressed as

$$\vec{E}_{\text{total}} = -\frac{\partial \vec{A}}{\partial t} - \nabla \phi = \vec{E}_i + \vec{E}_c \quad (3)$$

where \vec{A} is the vector magnetic potential (Wb/m) defined such that

$$\vec{B}_1 = \nabla \times \vec{A} \quad (4)$$

In order to reduce the absorbed power loss, \vec{E}_{total} should be minimized, but changes in E_i will necessarily require changes in the B_1 field distribution also. With a strategic arrangement of passive conductors, however, it is possible to implement a Faraday cage structure that cannot support significant circumferential RF electrical currents, and thus can reduce E_c in a solenoidal coil with minimal effect on the B_1 field [4].

3. Materials and methods

Numerical calculations were used to simulate and compare a variety of designs of E_c shield. To validate the numerical calculation

methods, experimental measurement of temperature increase in a phantom with and without an E_c shield was performed and results were compared to simulations.

3.1. Experimental setup

All MRI experiments were performed on a 14.1 tesla (600 MHz) Direct Drive spectrometer (Varian, Palo Alto, CA) using a custom-made solenoidal coil (3 mm diameter and 4.5 mm length) consisting of four turns of 0.35 mm-diameter copper. The sample (10 mM NaCl in a 1.67 mm outer diameter glass tube) was inserted into a polyamide tube (outer diameter: 2.24 mm, length 10.8 mm) which was placed into the solenoidal coil. Five copper wires of 50 μm diameter (California Fine Wire, Grover Beach, CA) oriented parallel to the axis of the coil were glued onto the outside of the polyamide tube. The RF coil was immersed in a perfluorinated liquid (FC43, 3M, Minnesota) for magnetic susceptibility matching and thermal isolation (Fig. 1).

Estimation of temperature increases were performed using interlaced periods of RF heating and MRI temperature measurements using the proton reference frequency (PRF) method [11].

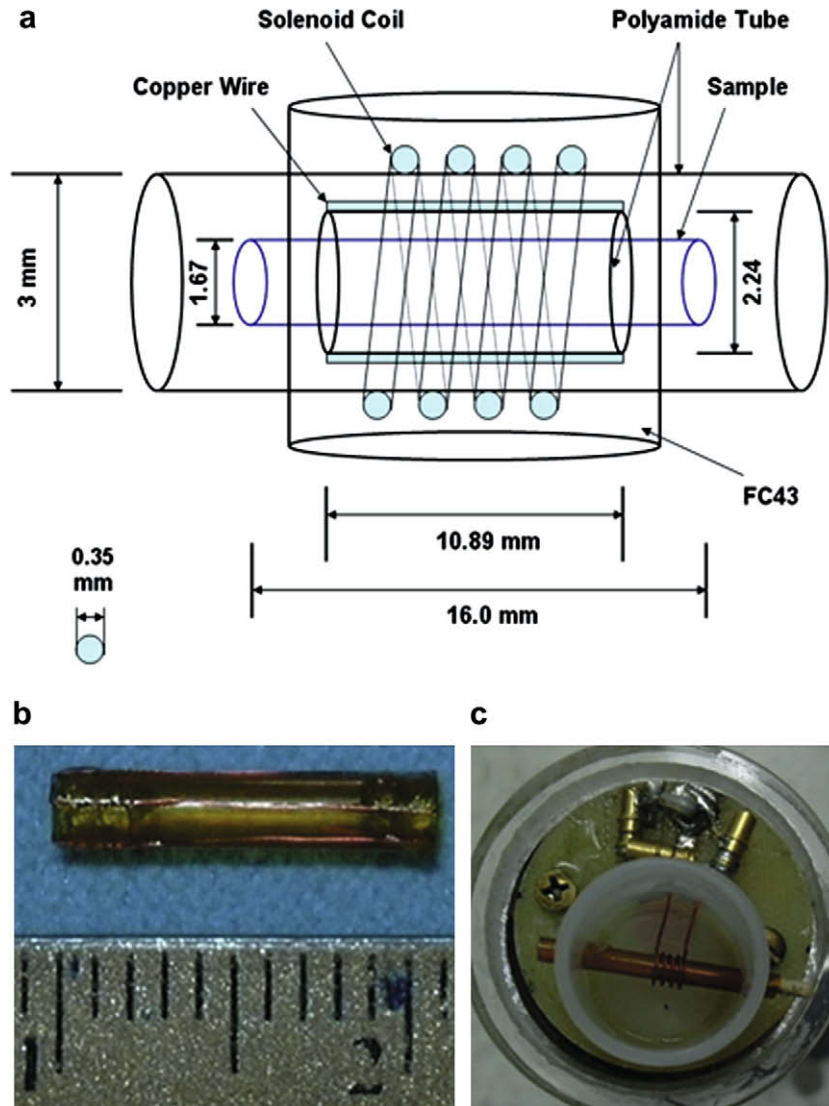


Fig. 1. The geometry of the solenoidal coil and copper wires for the experiment (a), the copper wires (b), and final assembly showing non-magnetic variable capacitors for impedance matching (c). Five copper wires were glued onto the outside of the polyamide tube to form an E_c shield, and FC43 (Perfluorotributylamine) was used for cooling of the solenoidal coil.

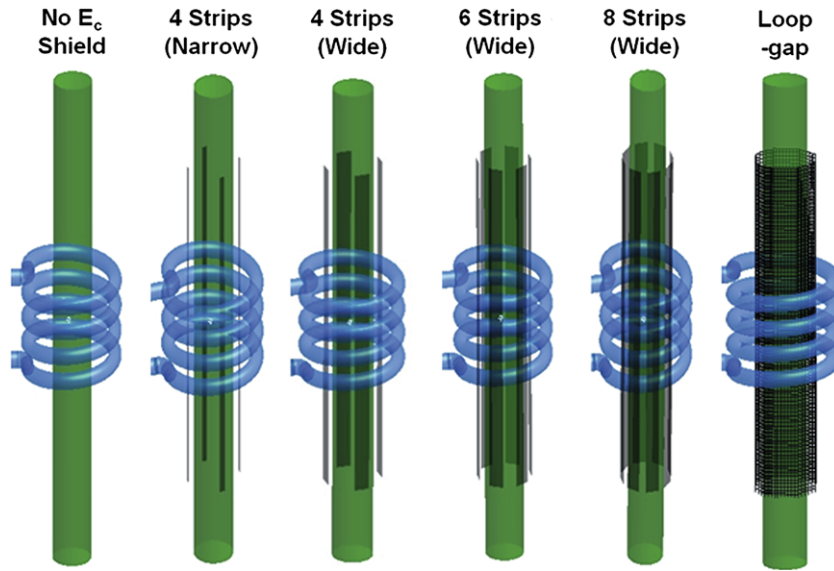


Fig. 2. Six different geometries used for the numerical calculations. E_c shields consisting of arrangements of narrow (200 μm width) or wide (600 μm width) copper strips each with length 10.8 mm were modeled. In addition, the case without any E_c shield served as a control, and for comparison a recently-published alternative, a loop-gap shield with diameter 2.4 mm and length 10.8 mm, was also modeled.

Five different time-average input powers (0, 0.15, 0.3, 0.6, and 1.2 W) were used for the heating periods. First, a baseline image was acquired using a single slice gradient-echo (GE) sequence (TR = 100 ms, TE = 10 ms, field-of-view = 20 \times 20 mm, matrix size = 256 \times 96, slice thickness = 1 mm, scanning time = 9.6 s). RF heating used a WALTZ-4 decoupling sequence which was applied for approximately 20 s. Imaging and heating procedures were successively repeated 16 times for each value of the input power. Phase difference images were generated using MATLAB (The MathWorks, Inc., Natick, MA), and phase unwrapping was performed using a previously-published method [12]. Temperature increases (ΔT) with respect to the baseline image were calculated according to [11]

$$\Delta T = -\frac{\Delta\phi}{0.01\gamma B_0 TE} \quad (5)$$

where $\Delta\phi$ is the difference in phase between the particular image and the baseline image acquired before the first heating period.

3.2. Numerical calculations

For comparison of the simulation to experimental results, the modeled coil and E_c shield geometries closely matched those used in experiment. Geometries with no E_c shield and with five copper strips of 50 μm width and 10.86 mm length placed between the solenoid coil and the sample were modeled. These models were defined on a rectilinear grid with 0.012 mm resolution for use with the finite difference time domain (FDTD) method of calculation for electromagnetics.

For numerical comparisons of different E_c shield designs, a model of a 1.6 mm-diameter, 16 mm-long 10 mM saline sample ($\sigma = 0.25/\text{m}$, $\epsilon_r = 78$ at 600 MHz) was created within the solenoid coil. Simulations with no E_c shield, and four different arrangements of evenly-spaced narrow copper strips (0.20 mm width, 10.8 mm length) or wider copper strips (0.60 mm diameter, 10.8 mm length), and a loop-gap shield [5] were performed with this arrangement. These models were defined on a rectilinear grid with 0.050 mm resolution for use with the FDTD method. These geometries are shown in Fig. 2.

All simulation work was performed using commercially-available FDTD software (xFDTD, Remcom, Inc., State College, PA), with

the coil driven by a sinusoidally-varying 600 MHz voltage source. Analysis of the results was performed in Matlab (The MathWorks, Inc., Natick, MA). All simulation results of electromagnetic fields were normalized so that $B_x = 4$ mT at the coil center.

To analyze calculation results, we applied a recently-developed method for separating E_c and E_i from the results of the FDTD calculation [13]. First, \vec{E}_i was calculated as

$$\vec{E}_i(r) = j\omega\vec{A}(r) = j\omega\frac{\mu_0}{4\pi} \int \int \int_r \frac{\vec{J}(r')}{|r-r'|} dv \quad (6)$$

where \vec{J} is the current density in the coil from the FDTD simulation, ω is the Larmor frequency, and μ_0 is the permeability of free space. \vec{E}_c was then calculated as

$$\vec{E}_c = \vec{E}_{\text{total}} - \vec{E}_i \quad (7)$$

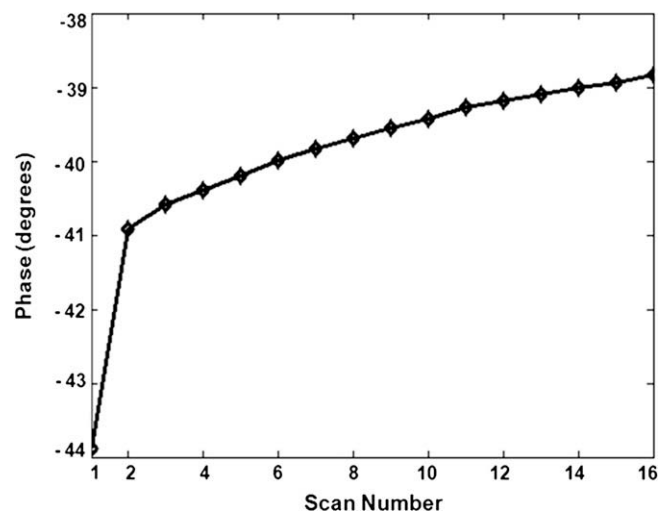


Fig. 3. Phase at the center of the sample throughout a single experiment involving a weak saline phantom (10 mM NaCl) without E_c shield and an input power of 1.2 W. Images corresponding to the first two data points would be used to make temperature maps because of weighting toward SAR effects and away from thermal conduction effects.

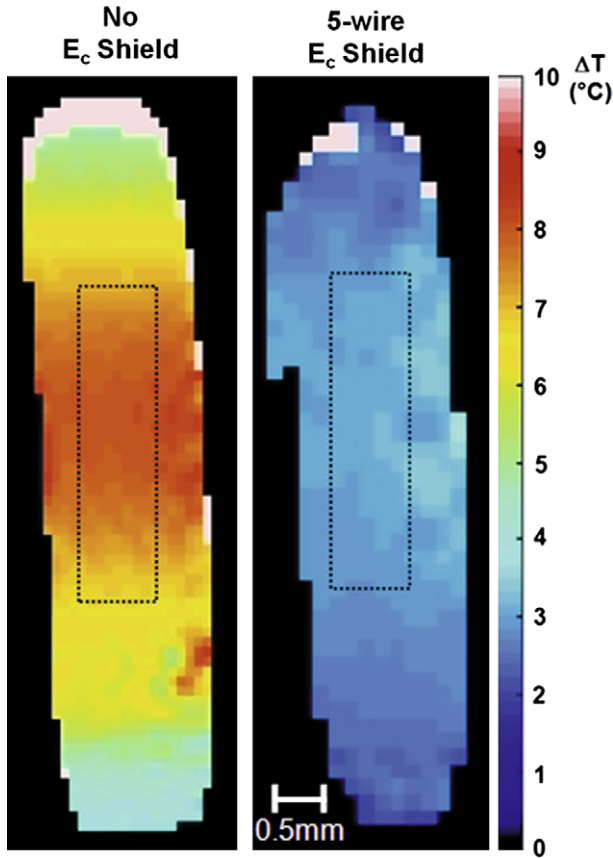


Fig. 4. Experimentally-measured temperature increase (ΔT) map within the saline sample (10 mM NaCl: $\sigma = 0.2$, $\epsilon_r = 78$) for different input power driving heating with (bottom) and without (top) copper wires. First two phase images were used to make phase difference map, which is necessary for the calculation of the ΔT image.

where \vec{E}_{total} is the electric field obtained from the FDTD simulation. This method is reasonably accurate when the currents in the coil are much greater than the currents in the sample and when the problem geometry is small enough that wavelength effects are negligible [13]: both conditions are well-satisfied by the experimental setups analyzed here.

4. Results

Fig. 3 shows the experimentally-measured increase in signal phase observed in a rectangular region of interest at the center of the phantom (see dotted line in Fig. 4) on gradient-echo images acquired between periods of heating when a time-average input power of 1.2 W is applied and no E_c shield is present. Most of the phase change (and thus temperature increase) occurs between the first (baseline) and second image, or during the first period of heating. After this, the effects of thermal conduction and mechanisms of heat transfer to the environment surrounding the sample become significant, and the temperature increases at a notably slower rate.

Fig. 4 shows maps of the experimentally-determined temperature increase in the phantom between the first (baseline) and second gradient-echo images with and without the presence of the 5-wire E_c shield when a time-average input power of 1.2 W is applied. The dotted rectangle outlines the region used for numerical data in Figs. 3 and 5 and in Table 1.

Table 1 and Fig. 5 present experimentally-measured temperature increases at the center of the phantom with and without the 5-wire E_c shield for a variety of input powers. The temperature in-

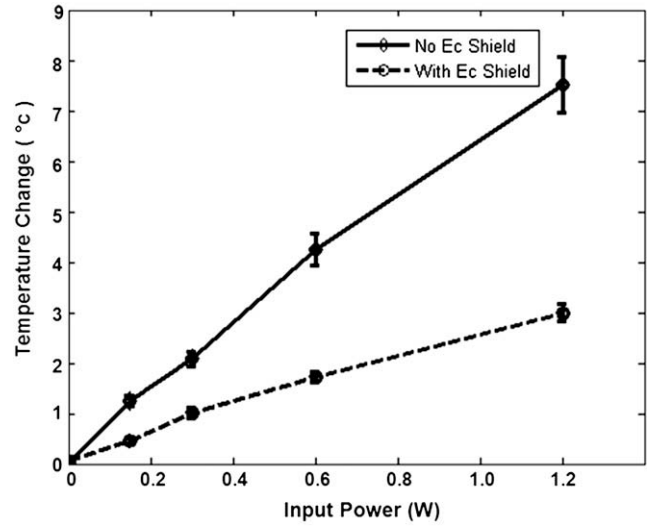


Fig. 5. Average temperature increase (ΔT) in the rectangular region of interest of the sample for different input powers without (solid) and with (dashed) copper wires. The temperature increase (ΔT) was decreased significantly with the addition of the copper wires. Error bars indicate standard deviation of temperature in region of interest.

crease is seen to be roughly proportional to the input power level. Values with no applied power during the heating period are close to zero, and indicate the level of error in the measurement. On average the temperature increase is reduced by approximately 58% with the addition of the 5-wire E_c shield in experiment.

Table 2 presents simulated values for the average E_c and B_1 fields, and standard deviation of the B_1 field with and without the 5-wire E_c shield. It is seen that the presence of the 5-wire E_c shield significantly reduces E_c with minimal effect on the B_1 field magnitude or homogeneity. Table 2 also gives the total power dissipated in the sample for each case, showing that the dissipated power is reduced by 57% with addition of the 5-wire E_c shield.

Fig. 6 shows the calculated magnitude of the E_c , E_i , and B_1 fields within the sample for six different simulation conditions including no E_c shield, four different arrangements of copper strips, and the loop-gap shield (geometries shown in Fig. 2). Table 3 gives numerical values for E_c and B_1 as well as the power dissipated in the sam-

Table 1

Experimentally-measured temperature change ΔT after 20 s of irradiation at different time-average input powers with and without the 5-wire E_c shield. With the E_c shield present, the temperature increase is approximately 60% smaller than when no E_c shield is present and RF power is applied.

Input power	0 W	0.15 W	0.3 W	0.6 W	1.2 W
Mean ΔT : No E_c shield	0.009 °C	1.25 °C	2.08 °C	4.24 °C	7.52 °C
Mean ΔT : 5-wire E_c shield	0.063 °C	0.47 °C	1.01 °C	1.72 °C	2.99 °C

Table 2

Numerically-calculated electromagnetic field properties with and without the 5-wire E_c shield. With the E_c shield present, the power dissipation is approximately 57% smaller than when no E_c shield is present, in good agreement with the experimentally-measured reduction of temperature increase.

	Sample Mean E_c (kV/m)	Sample Mean B_1^+ (mT)	Sample Std. B_1^+ (mT)	Sample Power Dissipation (mW)
No E_c shield	12.76	1.83	0.74	110.94
5-Wire E_c shield	8.53	1.83	0.74	48.05

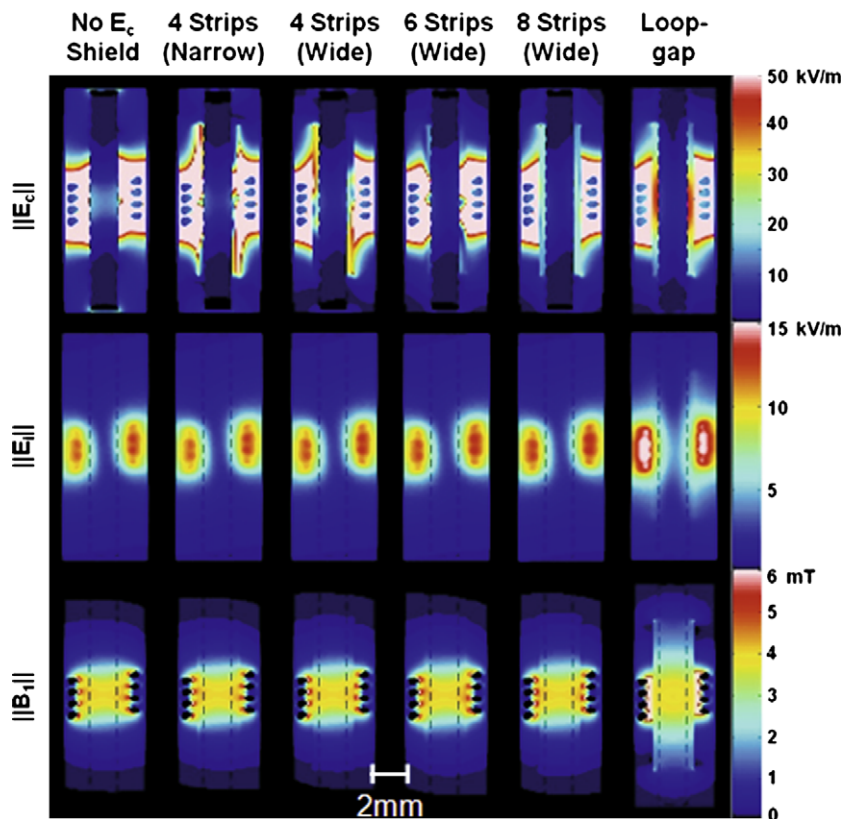


Fig. 6. Approximate magnitude of conservative electric field (E_c , first row), magnetically-induced electric field (E_i , second row), and total RF magnetic field (B_1 , third row) for six different conditions. All values were normalized so that $B_x = 4$ mT at the coil center.

ple for each case. The presence of any of the E_c shields is seen to reduce E_c and the dissipated power throughout the sample significantly. In all but the loop-gap shield this is accomplished with minimal effect on the B_1 field distribution. Of the geometries compared here, the 8-strip E_c shield reduces the dissipated power by the greatest amount (88%), with the 6-strip and loop-gap shield designs following closely.

5. Discussion

The results of this study confirm that strategically-placed passive conductors as an E_c shield can reduce RF heating of a sample within a solenoid coil. Although this general principle has been noted in, or can be inferred from, previous works [4,5], here numerical calculations are used to compare a number of designs, showing that the geometry of the E_c shield can largely determine its efficacy. For example, four narrow strips are shown to reduce power dissipation in the sample by 59%, but eight broad strips can reduce it by 88%.

Table 3

Calculated electromagnetic field properties within the sample between the two ends of the coil. SD indicates standard deviation. All values were normalized so that $B_x = 4$ mT at the coil center.

	Mean $\ E_c\ $ [kV/m]	Mean $\ B_1^z\ $ (mT)	SD $\ B_1^z\ $ (mT)	Power dissipation (mW)
No E_c shield	12.64	1.82	0.733	107.97
4 Strips (narrow)	8.84	1.82	0.732	44.48
4 Strips (wide)	7.30	1.82	0.732	24.59
6 Strips (wide)	6.26	1.83	0.735	13.72
8 Strips (wide)	6.20	1.83	0.733	12.81
Loop-gap shield	6.94	1.87	0.745	14.52

In general, a number of long, thin conductive strips or wires oriented parallel to the coil axis and placed on the outer surface of the cylindrical sample can reduce sample heating with minimal effect on the B_1 field, since the conductors can carry a charge density distribution opposing the E_c field of the coil, which is oriented along the coil axis [13], but cannot carry any significant current in the circumferential direction and thus cannot significantly affect the B_1 field of the solenoid. Another design, based on a single conductor around the surface of the cylinder – continuous except for one slit along its length oriented with the coil axis, the loop-gap shield [5] – has also been shown to significantly reduce heating, but with a significant effect on the magnitude and uniformity of the B_1 field. It was noted previously that the effect on the B_1 field is to make it more homogeneous along the whole length of a sample extending well beyond the ends of the solenoid [5]. This is also apparent in Fig. 6 of this work. However, in Table 3 we quantified the standard deviation of the B_1 field in the sample between the ends of the solenoid only, and found in that region the loop-gap shield did not improve homogeneity, but may actually slightly reduce it. Also, use of the loop-gap shield required approximately 40% greater current in the solenoid to achieve the same B_1 field magnitude at the center of the coil compared to the other cases. If the sample volume is significantly longer than the solenoid, this loss of sensitivity per sample volume at the center of the coil may be offset by greater sensitivity to regions of the sample outside the solenoid.

In principle, the use of E_c shields should also affect the signal-to-noise ratio (SNR). Reducing E_c in the sample reduces sample-related noise induced in the coil, but the addition of good conductors to the imaging volume also introduces a potential new source of noise. Careful analysis of this effect would require a different method for numerical calculation (such as a finite element method or a method of moments) which is more capable of accurately representing skin depth effects at the micron level. Work in this area is ongoing.

Acknowledgments

Funding for this work was provided by the National Institutes of Health (NIH) through R01 EB000454 and by the Pennsylvania Department of Health.

References

- [1] K.R. Minard, R.A. Wind, Solenoidal microcoil design – part II: optimizing winding parameters for maximum signal-to-noise performance, *Concepts Magn. Reson.* 13 (3) (2001) 190–210.
- [2] D.I. Hoult, P.C. Lauterbur, The sensitivity of the zeugmatographic experiment involving human samples, *J. Magn. Reson.* 34 (1979) 425–433.
- [3] B.S. Park, A.G. Webb, M.B. Smith, C.M. Collins, Conservative electric fields can dominate sample loss in high field microimaging, *ISMRM-ESMRMB* (2007) 3245.
- [4] D.G. Gadian, F.N.H. Robinson, Radiofrequency losses on NMR experiments on electrically conducting samples, *J. Magn. Reson.* 34 (1979) 449–455.
- [5] A. Krahn, U. Priller, L. Emsley, F. Engelke, Resonator with reduced sample heating and increased homogeneity for solid-state NMR, *J. Magn. Reson.* 191 (1) (2008) 78–92.
- [6] F.D. Doty, J. Kulkarni, C. Turner, G. Entzminger, A. Bielecki, Using a cross-coil to reduce RF heating by an order of magnitude in triple-resonance multinuclear MAS at high fields, *J. Magn. Reson.* 128 (2) (2006) 239–253.
- [7] P.L. Gor'kov, E. Chekmenev, C. Li, M. Cotten, J.J. Buffy, N.J. Traaseth, G. Veglia, W.W. Brey, Using low-E resonators to reduce rf heating in biological samples for static solid-state NMR up to 900 MHz, *J. Magn. Reson.* 185 (2007) 77–93.
- [8] J.A. Stringer, C.E. Bronnimann, G. Mullen, D.H. Zhou, S.A. Stellfox, Y. Li, E.H. Williams, C.M. Rienstra, Reduction of rf induced sample heating with a scroll coil resonator structure for solid state NMR probes, *J. Magn. Reson.* 173 (2005) 40–48.
- [9] B. Dillmann, K. Elbayed, H. Zeiger, M.-C. Weingertner, M. Piotta, F. Engelke, A novel low-E field coil to minimize heating of biological samples in solid-state multinuclear NMR experiments, *J. Magn. Reson.* 187 (2007) 10–18.
- [10] C.H. Wu, C.V. Grant, G.A. Cook, S.H. Park, S.J. Opella, A strip-shield improves the efficiency of a solenoid coil in probes for high-field solid-state NMR of lossy biological samples, *J. Magn. Reson.* 200 (2009) 74–80.
- [11] K. Kuroda, K. Abe, S. Tsutsumi, Y. Ishihara, Y. Suzuki, K. Satoh, Water proton magnetic resonance spectroscopic imaging, *Biomed. Thermol.* 13 (1994) 43–62.
- [12] M. Jenkinson, Fast, automated, N-dimensional phase-unwrapping algorithm, *Magn. Reson. Med.* 49 (2003) 193–197.
- [13] B. Park, A.G. Webb, C.M. Collins, A method to separate conservative and magnetically-induced electric fields in calculations for MRI and MRS in electrically-small samples, *J. Magn. Reson.* 199 (2009) 233–237.